

RESEARCH ARTICLE

Global changes in gene expression during compatible and incompatible interactions of faba bean (*Vicia faba* L.) during *Orobanche foetida* parasitism

Amal Boukteb^{1,2}, Kazuki Sato³, Pamela Gan³, Mohamed Kharrat², Hanen Sakouhi², Arisa Shibata³, Ken Shirasu³, Yasunori Ichihashi⁴, Mariem Bouhadida^{1,2*}

1 Faculty of Science of Tunis, University of Tunis El Manar, Tunis, Tunisia, **2** Field Crop Laboratory, National Institute of Agricultural Research of Tunisia, Carthage University, Tunis, Tunisia, **3** RIKEN Center for Sustainable Resource Science, Yokohama, Japan, **4** RIKEN BioResource Research Center, Tsukuba, Japan

* mariem.bouhadida@inrat.ucar.tn



OPEN ACCESS

Citation: Boukteb A, Sato K, Gan P, Kharrat M, Sakouhi H, Shibata A, et al. (2024) Global changes in gene expression during compatible and incompatible interactions of faba bean (*Vicia faba* L.) during *Orobanche foetida* parasitism. PLoS ONE 19(4): e0301981. <https://doi.org/10.1371/journal.pone.0301981>

Editor: Giannantonio Domina, University of Palermo, ITALY

Received: October 6, 2023

Accepted: March 26, 2024

Published: April 16, 2024

Copyright: © 2024 Boukteb et al. This is an open access article distributed under the terms of the [Creative Commons Attribution License](https://creativecommons.org/licenses/by/4.0/), which permits unrestricted use, distribution, and reproduction in any medium, provided the original author and source are credited.

Data Availability Statement: The data that support the findings of this study are openly available in NCBI's Sequence Read Archive (SRA) at <https://www.ncbi.nlm.nih.gov/sra/PRJNA1023273>, reference number PRJNA1023273.

Funding: The Ministry of Higher Education and Scientific Research of Tunisia and the Ministry of Agriculture of Tunisia provided a financial support for this study to AB and MB. The "Société de Promotion du Lac du Tunis" provided a financial

Abstract

Orobanche foetida Poiret is the main constraint facing faba bean crop in Tunisia. Indeed, in heavily infested fields with this parasitic plant, yield losses may reach 90%, and the recent estimation of the infested area is around 80,000 ha. Identifying genes involved in the *Vicia faba*/*O. foetida* interaction is crucial for the development of effective faba bean breeding programs. However, there is currently no available information on the transcriptome of faba bean responding to *O. foetida* parasitism. In this study, we employed RNA sequencing to explore the global gene expression changes associated with compatible and incompatible *V. faba*/*O. foetida* interactions. In this perspective, two faba bean varieties (susceptible and resistant) were examined at the root level across three stages of *O. foetida* development (Before Germination (BG), After Germination (AG) and Tubercule Stage (TS)). Our analyses presented an exploration of the transcriptomic profile, including comprehensive assessments of differential gene expression and Gene Ontology (GO) enrichment analyses. Specifically, we investigated key pathways revealing the complexity of molecular responses to *O. foetida* attack. In this study, we detected differential gene expression of pathways associated with secondary metabolites: flavonoids, auxin, thiamine, and jasmonic acid. To enhance our understanding of the global changes in *V. faba* response to *O. foetida*, we specifically examined WRKY genes known to play a role in plant host-parasitic plant interactions. Furthermore, considering the pivotal role of parasitic plant seed germination in this interaction, we investigated genes involved in the orobanchol biosynthesis pathway. Interestingly, we detected the gene expression of VuCYP722C homolog, coding for a key enzyme involved in orobanchol biosynthesis, exclusively in the susceptible host. Clearly, this study enriches our understanding of the *V. faba*/*O. foetida* interaction, shedding light on the main differences between susceptible and resistant faba bean varieties during *O. foetida* infestation at the gene expression level.

support for this study to AB. The Ministry of Education, Culture, Sports, Science and Technology of Japan provided a financial support for this study to KS [KAKENHI grants (21H02506)]. The funders had no role in study design, data collection and analysis, decision to publish, or preparation of the manuscript.

Competing interests: The authors have declared that no competing interests exist.

Introduction

Faba bean (*Vicia faba* L., $2n = 12$) is one of the oldest legume crops which has been domesticated more than 10,000 years BP [1,2]. It has been cultivated for its high protein content in human diets, as well as for animal fodder and forage [3]. Currently, the global production of faba bean is around 5,964,384 t grown on 2,722,690 ha [4]. Faba beans are also recognized for their ability to fix atmospheric nitrogen [5]. Therefore, faba bean could be used to reduce the need for nitrogen fertilizer applications through land rotation [6], intercropping to enrich soil [7], and as a companion crop to increase the yield of other plants, such as barley [8] and wheat [9–11].

In Tunisia, faba beans occupy an area of 53,820 ha (DGPA, 2021). This area represents about 72% of all food legumes areas in Tunisia with a predominance of minor type (about 62%) compared to major type (38%) [12]. This difference on faba beans superficies could be explained by the fact that the minor type releases more nitrogen on the soil than the major type. Indeed, in Tunisia, the minor type is cultivated to improve the productive performance of the cereal system and to produce a source of local protein for animal nutrition [13].

The main constraint facing faba bean crop, in Tunisia, is the infestation with parasitic plants, mainly broomrapes. These parasitic plants have an exceptional fertility that gives rise to 50,000 to 500,000 seeds/plant. These seeds can remain viable for up to 20 years or more in the absence of the host [14], which causes major damage that severely reduces crop yields up to a total loss [15]. The broomrape infestation in many countries that exploit food legumes has forced them to become importers of their agricultural products to satisfy local demand. In Tunisia, in heavily infested fields, yield losses may reach 90% [16,17], and the recent estimation of the infested area is around 80,000 [18].

Awareness of the *Orobanche* threat to faba bean production in Tunisia is not recent; it was first described a century ago by Boeuf [19] as a real danger, to the point that he suggested, in some cases, giving up on cultivating faba bean. Two *Orobanche* species were noticed by Chabrolin [20] on faba bean field, *O. foetida* Poirlet and *Orobanche crenata* Forsk (called at that time *Orobanche speciosa*). The *O. crenata* was the main constraint on faba bean crop in Tunisia, while *O. foetida* was observed with insignificant damage. However, since 1992, *O. foetida* has become a real threat causing severe damages in Tunisia mainly on faba bean [21]. *Orobanche foetida*, a holoparasitic plant, was firstly described in North Africa by Poirlet during his travels in ancient Numidians between 1785 and 1786 [22]. It is a tetraploid plant ($2n = 4x = 76$) [23,24], characterized by an intense red color and a foul odor. Currently, the *O. foetida* is detected on different crops such as chickpea (*Cicer arietinum*), grass pea (*Lathyrus sativus*), lentil (*Lens culinaris*), vetch (*Vicia sativa*) and fenugreek (*Trigonella foenum-graecum*) [25,26]. It is distributed mainly in the North West of Tunisia [27]. Moreover, it is important to mention that populations of *O. foetida* are more aggressive on faba bean than on other food legume crops [28]. Additionally, we demonstrated in a previous study that Tunisian populations of *O. foetida* attacking faba bean did not display any strong clustering pattern suggesting that they belong to the same gene pool [27]. Although *O. foetida* has been reported only in Spain, Portugal and Morocco attacking mainly wild legumes [29,30]. In fact, *O. foetida* presents a potential threat to legume crops due to its ability to parasitize a wide spectrum of hosts [31].

Obligate parasitic plants, devoid of chlorophyll, are totally depending on their hosts for their growth. The germination of these parasite seeds only occurs after the perception of germination stimulants released into the root exudates by the host. These host-derived chemicals belong mainly to the strigolactones (SLs) family. The first described SLs was strigol as a germination stimulant for *Striga*, isolated from the root exudates of a false host, cotton (*Gossypium hirsutum*) [32]. Later, the orobanchol was identified as the first *Orobanche* germination

stimulant from red clover (*Trifolium pratense*) root exudates [33]. To date, more than 30 SLs have been characterized mainly as germination stimulants for root parasitic weeds [34]. The germination of *Orobancha* seeds is followed by the development of the radicle [15]. Thereafter, parasitic plants ensure their invasion of the host via a specialized organ called “haustorium”, which attaches and penetrates the root or stem of the host [35]. Thus, a new organ called “tubercle” develops on the host’s root and acts as a strong well to accumulate reserves [36]. This phase of the *Orobancha* life cycle is occurring underground. Hence, the presence of these parasites can only be detected after the emergence of a stem above the ground, leading the development of the inflorescence.

Defense mechanisms deployed by the host against *Orobancha* attack are coordinated within the evolution of the parasitic plants’ invasion into its tissues. Early resistance mechanisms involve, mainly, a low induction of seed germination by host roots [37]. Later, upon the vascular connections through the haustorium, various responses include the induction of immunity-related genes; the production of ROS, the deposition of callose, the occlusion of vessels, as well as a localized hypersensitive response (HR) [38–40]. The post-attachment resistance consists, mainly, of parasitic necrosis due to the occlusion of the host vessel by mucilage or the production of toxic compounds [37,41,42]. Throughout the interaction, the host defends itself by activating signaling pathways involving phytohormones, jasmonic acid (JA), salicylic acid (SA), and ethylene (ET) [15].

Identifying genes involved in the *V. faba/O. foetida* interaction is crucial for the development of effective faba bean breeding programs. However, there is currently no available information on the transcriptome of faba bean responding to *O. foetida* parasitism. Additionally, very limited genomics resources are available regarding faba bean genome. Therefore, the objective of this study is to explore global gene expression changes that occur during compatible and incompatible *V. faba/O. foetida* interaction, using RNA sequencing (RNA-seq). Indeed, RNA-seq allows a comprehensive characterization of gene expression within a particular tissue under specific conditions without requiring a reference gene set. Evidently, the present study contributes to our understanding of *V. faba/O. foetida* interaction by revealing key differences between resistant and susceptible faba bean varieties, at gene expression level, during *O. foetida* infestation. This knowledge will provide valuable insights for identifying potential targets genes that could be useful for developing resistant faba bean varieties against *O. foetida* attack.

Materials and methods

Experimental design

In this study, we used two faba bean varieties released by the Tunisian breeding program: the variety ‘Badii’ (S_Host) widely grown in the main faba bean cropping areas in Tunisia and known for its high susceptibility to *O. foetida*, thus it is largely used as a susceptible check; and the resistant variety ‘Chourouk’ (R_Host) recently released to better face *O. foetida* attack in the high infested fields [17]. The resistance of the ‘Chourouk’ variety is evident through the absence of *O. foetida* seed germination. This choice allows us to investigate and compare their gene expression responses at the molecular level. We collected faba bean roots at different stages of *O. foetida* development; Before Germination (BG), After Germination (AG), and Tubercle Stage (TS). Three replications were performed for each condition per host. The collected roots were washed thoroughly with tap water and stored on Liquid Nitrogen at -80°C. Samples were, then, freeze-dried until needed. In total, we collected 36 samples including S_Host and R_Host roots at the three selected stages of *O. foetida* development (BG,AG, TS) in the two conditions infected and not-infected by *Orobancha* seeds.

In vitro co-culture & sample collection

The connection between the broomrape and its host occurs underground, which does not allow us to easily observe this interaction. To track the progress of the parasitism cycle and to facilitate sample collection, we adopted the hydroponic *in vitro* co-culture *V. faba*/*O. foetida* system [37] (Fig 1A). Indeed, *O. foetida* seeds were displayed in the presence of faba bean roots as follows; Firstly, *Orobanche* seeds (20 mg) were surface-sterilized for 5 min in sodium hypochlorite $\text{Ca}(\text{ClO})_2$ (1%), rinsed four times (2 min) with sterile distilled water and kept at 25°C for 10 days for preconditioning. Then, faba bean seeds were also surface-sterilized in sodium hypochlorite $\text{Ca}(\text{ClO})_2$ (5%) for 15 min, followed by three washings (5 min) in sterile distilled water. Faba bean seeds were then sown in sterile sand and kept in the dark at room temperature for 4 days. Secondly, we prepared squared Plastic petri dishes/plates (120*120, 4 vents, Laboratory Disposables by Biosphere Biomedical Technics, Sfax, Tunisia) as support by applying three perforations in the two opposite borders of the Petri dish, one on the top to allow the growth of the faba bean stem and the two others on the right and the left corners on the bottom of the Petri dishes to allow root feeding in culture medium. Thirdly, we filled the dishes with sterile sand and covered them with filter paper. Finally, faba bean seeds with a radicle of 4–5 cm in length were deposited on the filter paper with the *Orobanche* seeds already spread on the paper. Dishes were covered with aluminum foil to exclude light from the roots and were placed vertically in boxes. The experimental set-up was maintained in a greenhouse at 25°C with 78% humidity. All the above steps were performed under sterile conditions.

To track the evolution of *V. faba*/*O. foetida* interaction, weekly observations were conducted using a binocular stereoscope. Prior to *O. foetida* seed germination, the initial set of faba bean roots were collected (BG: Before Germination). Upon detecting germination of *O.*

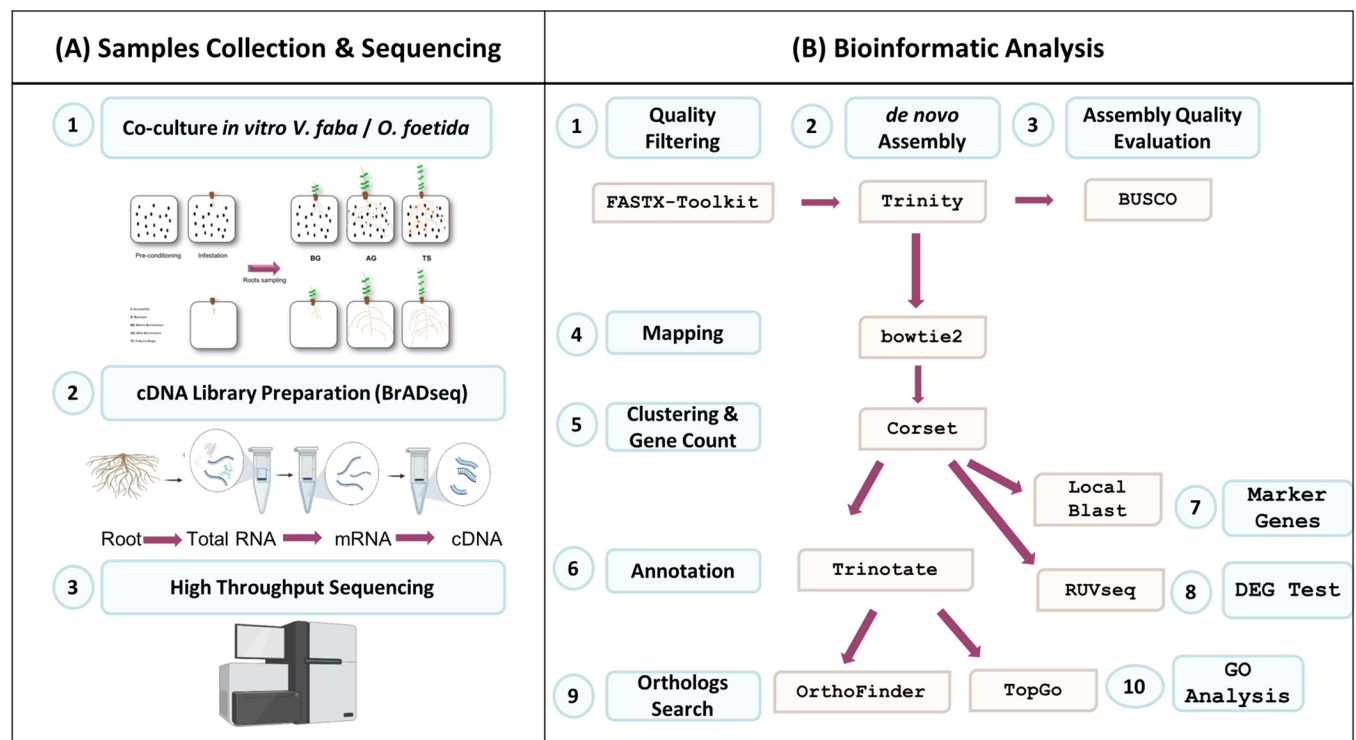


Fig 1. Overall pipeline for *Vicia faba* root gene expression during *Orobanche foetida* attack from (A) sample collection to (B) bioinformatic analysis.

<https://doi.org/10.1371/journal.pone.0301981.g001>

foetida, faba bean roots were meticulously gathered (AG: After Germination). Subsequent observations tracked the tubercle development (TS: Tubercle Stage), leading to a third collection of faba bean roots.

mRNA extraction, library preparation & sequencing

Firstly, we extracted total RNAs from freeze-dried roots (Fig 1A). We homogenized the collected samples with liquid Nitrogen and we performed a total RNAs extraction using RNeasy Plant Mini Kit (Qiagen, Hilden, Germany) following the manufacturer's instructions. RNA quality and quantity control of total RNA samples was carried out using NanoDrop One Microvolume UV-Vis Spectrophotometers (Thermo Fisher Scientific, Massachusetts, USA). Secondly, we performed mRNA extraction and library preparation using BrADseq Protocol [43] by applying "Option A—mRNA random octamer-adapter priming (SHO)" during "3' Adapter cDNA Priming" step since we are working with a non-Model Plant. Then, we checked the mRNA quality using Bioanalyzer (Agilent, CA, USA). Libraries were multiplexed and pooled, concentration was estimated using Multimode Microplate Readers (Infinite 200 Pro, Mannedorf, Switzerland). Finally, we conducted a Paired-end sequencing using the Illumina NextSeq500/550 Mid-Output v2 Kit (Illumina, CA, United States).

De novo assembly

Prior to analyses, raw paired-end reads were quality-filtered using the Fastx toolkit (http://hannonlab.cshl.edu/fastx_toolkit/index.html) to remove adapter sequences (fastx_trimmer), low-quality nucleotides from the end of the reads, short reads (fastq_quality_trimmer), and low-quality reads (fastq_quality_filter) by fixing the Phred score at 33 (Fig 1B). In order to perform a comprehensive comparison between susceptible and resistant hosts, we independently performed two distinct *de novo* assemblies using Trinity v2.0.6 [44] [*parameters:—max_memory 50G —SS_lib_type FR*] (Fig 1B). Each assembly was conducted separately for the respective host, employing pooled sequence data.

The assembled transcriptomes were assessed for completeness through the gVolante v.1.2.0 [45] web server with BUSCO v2/v3 [46], using a plant database of 1,440 genes (Fig 1B). To align the reads against the *de novo* assembled transcriptome, the sequences were processed with Bowtie2 v. 2.3.5 [47]. Furthermore, we used Corset software [48], a method that hierarchically clusters contigs using shared reads and expression, for obtaining gene-level counts from any *de novo* transcriptome assembly (Fig 1B). Each cluster is defined as a unigene, thus, unigenes were used for subsequent annotations. The gene-level counts can then easily be tested for differential expression using count-based frameworks [48]. The corset software was utilized with default parameters.

Differential gene expression

To identify Differentially Expressed Genes (DEGs), we used gene-level counts generated by Corset structuring our analysis, to reveal gene expression patterns across specific developmental stages (BG, AG, TS) for both hosts. Our DEG detection strategy employed negative binomial generalized linear modeling (GLM) analysis. Initially, we calculated normalization factors using the trimmed mean of M-values (TMM) method. To address potential batch effects and unwanted variations, our analysis integrated the Remove Unwanted Variation using the RUVg method [49]. A GLM likelihood ratio test (LRT) was conducted to identify differentially expressed genes among the designated groups. The identification of DEGs, characterized by a false discovery rate (FDR) ≤ 0.05 and a log-transformed fold change (logFC) ≥ 0 or $\logFC \leq 0$, was performed through the quasi-likelihood F-test. This, involved comparing

expression levels during infection and non-infection by *O. foetida* at the same time points (BG, AG, TS) for both hosts. Our methodology ensured a robust and comprehensive approach to unraveling the dynamic changes in gene expression associated with *O. foetida* infection across distinct developmental stages and hosts.

Functional annotation of unigenes

We analyzed the unigenes using Trinotate pipeline following the method outlined at (<http://trinotate.github.io/>) (Fig 1B). For a better understanding of the genes implicated in the *V. faba*/*O. foetida* interaction, particularly from the host's perspective, we conducted a Blastx analysis targeting two crucial sets of proteins: the WRKY family and those associated with the orobanchol biosynthesis pathways. The selection of the WRKY family was motivated by previous findings indicating their involvement in the *Helianthus annuus*/*Orobancha cumana* interaction [50]. Regarding the orobanchol proteins, we focused on germination stimulants. This choice was guided by previous observations showing that *O. foetida* seeds failed to germinate in the presence of the resistant host, leading us to specifically investigate genes related to the orobanchol pathway [51]. The proteins list used for this analysis is represented in the supplementary materials (S1 and S2 Tables).

Gene ontology. We conducted a Gene Ontology (GO) enrichment analysis (Fig 1B) using the "topGO" R package [52]. The procedure involved incorporating the results of the differential expression analysis and the GO term assignments from Trinotate to identify GO terms based on their expression patterns in the different studied stages (BG, AG, and TS of *O. foetida* development) for both hosts (S_Host and R_Host). The enrichment *p*-values were calculated using the "elimFisher" method.

Ortholog search. We carried out an Ortholog search using OrthoFinder [53] (Fig 1B), a phylogenetic orthology inference method for comparative genomics. Orthofinder requires only protein sequences file in FASTA format for each study species. In the present study, we used the protein files generated by TransDecoder for both hosts (S_Host and R_Host) during Trinotate analysis.

Primers design and PCR amplification

In the present study, our focus is, identifying molecular distinctions as potential targets for releasing new *V. faba* resistant varieties to *O. foetida* attack. With this in perspective, we specifically interested into genes' profile associated with the orobanchol biosynthesis pathway. After an assessment of the expression of these genes in both susceptible and resistant hosts, we conducted a PCR experiment to verify the presence of non-expressed genes within the *Vicia faba* genome. First, we designed specific primers for 4 genes: AtMAX1, MtMAX1B, VuCYP722C and OsCYP711A3. Briefly, we performed a mapping of transcripts against the gene to identify the target sequences. Then, we designed Primer pairs (Table 1) using Primer3 (<https://primer3.ut.ee/>) while ensuring avoidance of off-target binding. Second, we extracted the DNA from each host following a modified CTAB method [54]. Third, we carried out the PCR amplification as following: The 50 μ L PCR amplification system included 2.0 μ L of template DNA, 5.0 μ L of 10X PCR buffer, 1.0 μ L of dNTPs (2.5 mM), 1.5 μ L of MgCl₂, 1.0 μ L of each Left and Right primer (1 M), and 0.4 μ L of Taq polymerase (2 U/ μ L). Finally, ddH₂O was added to complete the 50 μ L. The PCR amplification process involved 30 cycles of denaturation at 94°C for 30 seconds, annealing at 55–61°C for 30 seconds, extension at 72°C for 30 seconds, and a final extension step at 72°C for 7 minutes.

Table 1. Primers list designed for PCR.

		Length (nt)	Tm (°C)	%GC	Sequences
MtMAX1B	Left Primer	21	57.99	47.62	GCCCCACTCATTTCATTCTTCT
	Right Primer	21	58.79	47.62	GCAAGGACTGAGAAAACGTCA
CYP722C	Left Primer	21	57.89	52.38	GGCACACATACCTAGGCTAAG
	Right Primer	21	57.58	42.86	AGCAGCTGGTTATTCTTGTGA
Os1400	Left Primer	20	58.94	50.00	ACCTCTGCTTACTGGTGCTT
	Right Primer	22	58.69	45.45	ACTCCACTCTTTACAGGAACCA
AtMAX1	Left Primer	22	57	45	CTCGATCAGGTGCTTCATTAGT
	Right Primer	23	57	39	AGTGTGCTGACTGTAATGGACTAA

<https://doi.org/10.1371/journal.pone.0301981.t001>

Results

In this study, we adopted the *in vitro* co-culture system in order to easily track the progress of *V. faba*/*O. foetida* interaction. We observed the germination of *O. foetida* seeds in the presence of the susceptible host (S_Host), whereas *O. foetida* germination was absent with the resistant host (R_Host), indicating the early resistance mechanism at the pre-attachment phase.

De novo assembly

To characterize the transcriptome of two *V. faba* varieties (S_Host and R_Host) root during *O. foetida* infection, we sequenced corresponding cDNA libraries using the Illumina sequencer. After a series of filtering of the pooled reads, we counted a total of 33,442,981 reads for the S_Host and 27,641,999 reads for the R_Host. Both transcriptomes of two *V. faba* varieties were assembled using Trinity, generating 106,178 and 72,526 contigs with an average length around 510 nt and 493 nt for S_Host and R_Host respectively (Table 2). The distribution of the length of the contigs of the two transcriptomes showed that there was no strength difference between both transcriptomes: the majority of the contigs counts around 300 nt, while relatively few contigs were ranging from 1,000 to 2,000 nt in length (Fig 2). Besides, we assessed the accuracy and completeness of the two assemblies using BUSCO, suggesting that both host genomes have a fraction of genes that are well-represented and fully reconstructed in the assemblies. We detected 35% complete genes in S_Host and 23% in R_Host assemblies.

Table 2. *De novo* assembly statistics for the susceptible (S_Host) and the resistant (R_Host) hosts transcriptomes.

	S_Host	R_Host
Number of contigs	106178	72526
Total size of contigs (nt)	54176411	35741324
N50 contig length (bp)	633	592
Average length of contigs(nt)	510	493
Median length of contigs(nt)	342	347
Minimum length of contigs(nt)	201	201
Maximum length of contigs(nt)	6299	5867
Base composition (%)	A:29.53, T:30.63, G:21.39, C:18.45	A:29.28, T:30.29, G:21.70, C:18.73
GC-content (%)	39.84	40.43
Complete genes	506 (35.14%)	327 (22.71%)
Complete genes + Partial	796 (55.28%)	520 (36.11%)
Missing core genes	644 (44.72%)	920 (63.89%)
Total BUSCO groups searched	1440	1440

<https://doi.org/10.1371/journal.pone.0301981.t002>

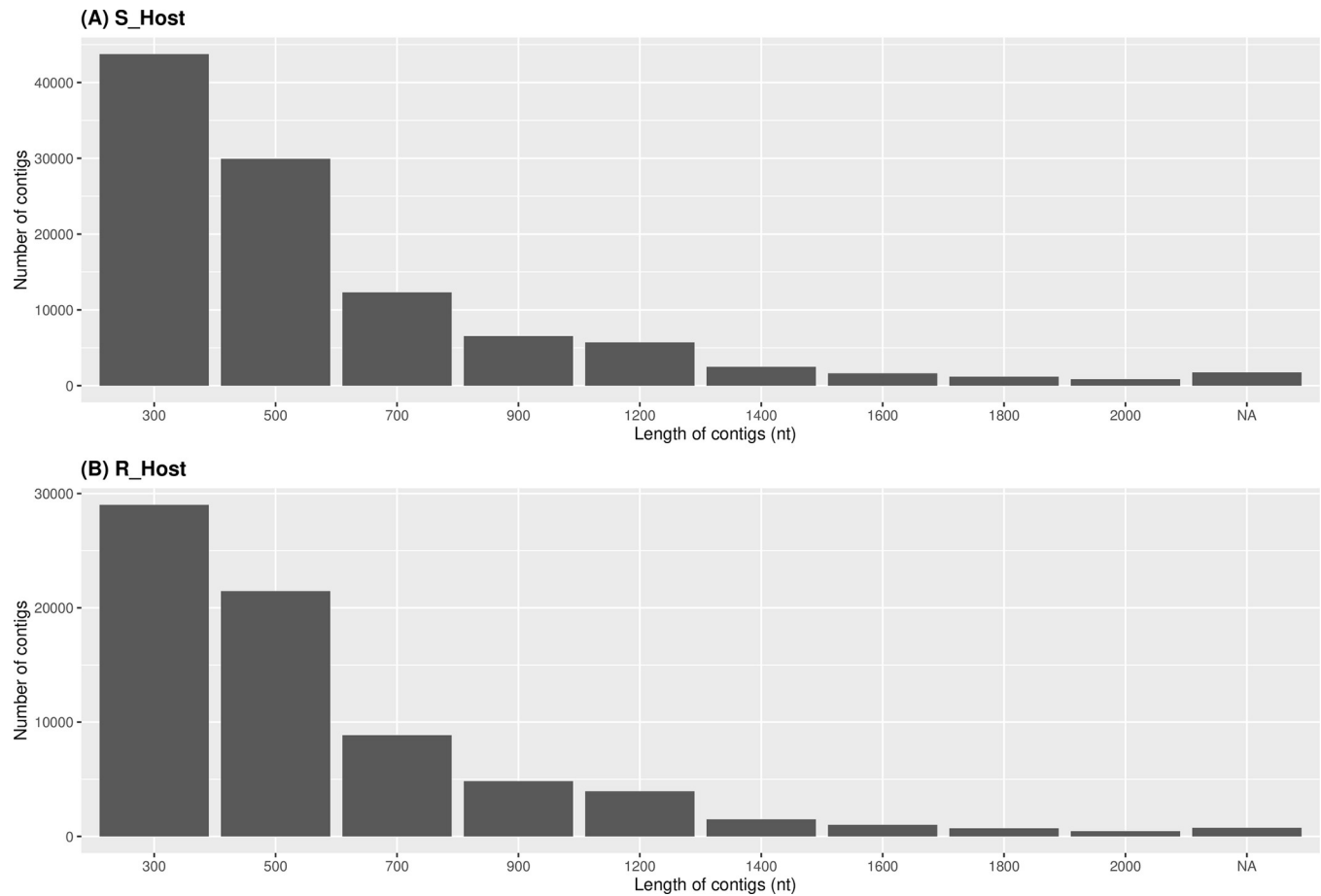


Fig 2. Distribution of the length of the contigs obtained by the *de novo* assembly of the transcriptome sequencing in two *Vicia faba* varieties. A susceptible (S_Host) (A) and a resistant (R_Host) (B) against *Orobanche foetida* attack.

<https://doi.org/10.1371/journal.pone.0301981.g002>

The OrthoFinder analysis comparing S_Host and R_Host to *O. foetida* parasitism highlights that both hosts share conserved functions (100%) in orthogroups containing species genes (Table 3). Moreover, the presence of only a few species-specific orthogroups could be attributed to the comparison between two varieties belonging to the same species.

Table 3. Summary of the Orthofinder analysis for the susceptible (S_Host) and the resistant (R_Host) hosts transcriptomes.

	S_Host	R_Host
Number of genes	35013	27148
Number of genes in orthogroups	21782	20523
Number of unassigned genes	13231	6625
Percentage of genes in orthogroups	62.2	75.6
Percentage of unassigned genes	37.8	24.4
Number of orthogroups containing species	17206	17208
Percentage of orthogroups containing species	100.0	100.0
Number of species-specific orthogroups	5	7
Number of genes in species-specific orthogroups	24	29
Percentage of genes in species-specific orthogroups	0.1	0.1

<https://doi.org/10.1371/journal.pone.0301981.t003>

Analysis of differential expressed genes

To identify the differentially expressed genes (DEG) between infected and non-infected faba bean with *O. foetida*, we analyzed the gene-level counts matrix generated by Corset software using the RUVseq package in R software [49]. A total of 622 unigenes were identified as differentially expressed in S_Host among the three studied stages (BG, AG, TS), while 381 unigenes were detected for R_Host. Moreover, we observed shared differentially expressed unigenes only within S_Host among the three stages (Fig 3). Furthermore, for both hosts, we observed

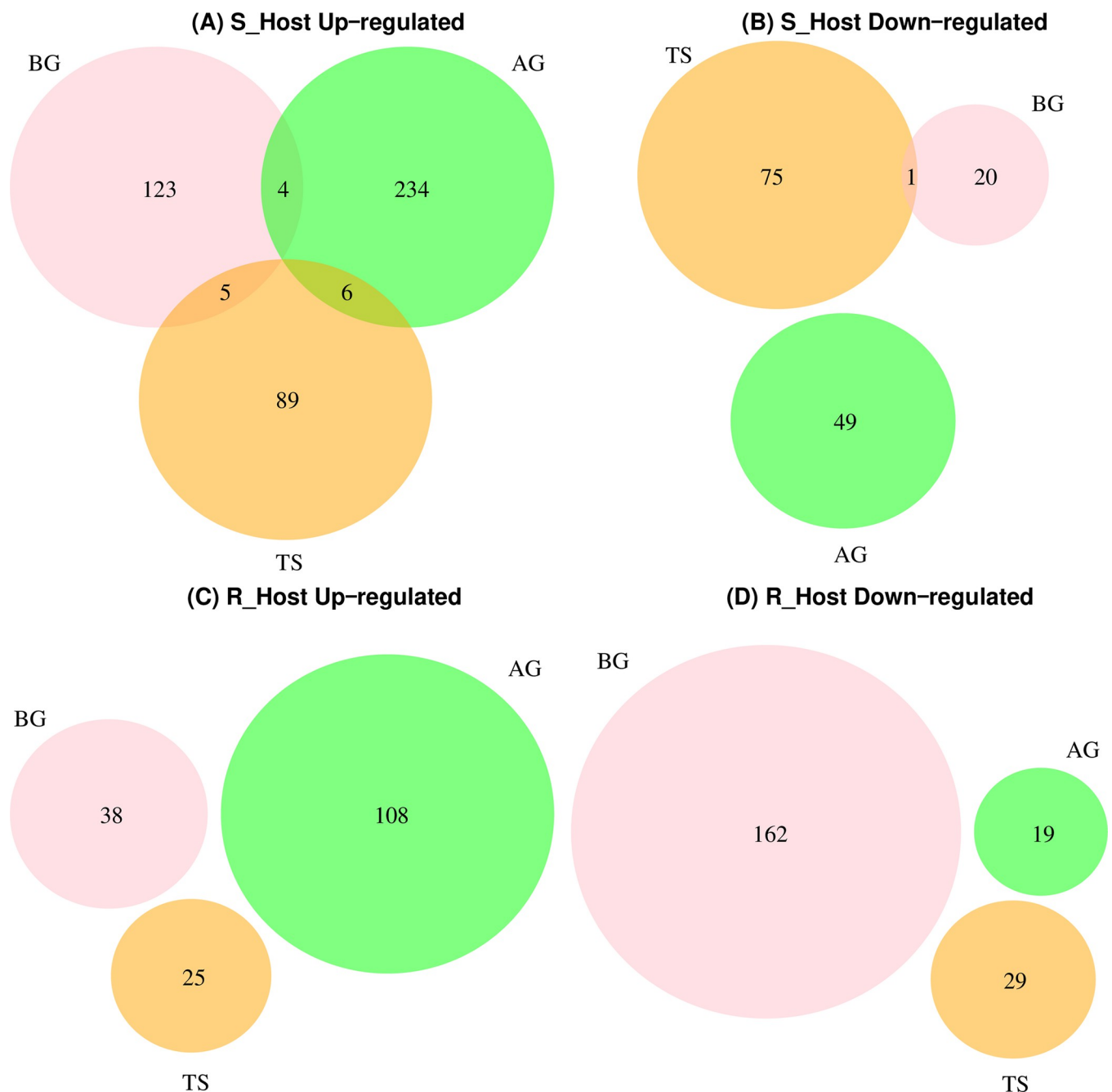


Fig 3. Venn diagram representing the significantly differentially expressed unigenes in two *Vicia faba* varieties comparing samples infected and non-infected by *Orobanche foetida* seeds. A susceptible (S_Host) (A, B) and a resistant (R_Host) (C, D) against *O. foetida* attack.

<https://doi.org/10.1371/journal.pone.0301981.g003>

the highest number of up-regulated unigenes during the After Germination stage (AG) [S_Host = 234; R_Host = 108], while the lowest numbers were observed at Tubercle Stage (TS) [S_Host = 89; R_Host = 25] (Fig 3A and 3C). Additionally, we detected the highest number of down-regulated unigenes (162) at the BG stage in R_Host (Fig 3D), while only 20 were detected at the same stage in S_Host (Fig 3B). Moreover, our investigation revealed that orthologous genes differentially expressed in one host are largely insignificant in the other, emphasizing host-specific responses.

Functional annotation

Go enrichment analysis. To understand the biological functions of the identified DEGs, we performed a GO enrichment analysis using the topGO R package [52]. Accordingly, we constructed the bubble plots to visualize the GO terms of the Biological Process category (Figs 4 and 5) associated with specific DEGs for both hosts (S_Host, R_Host) at the studied stages (BG, AG, TS). We chose to represent the Top 25 of GO terms enriched in the DEGs for S_Host and R_Host, respectively, although the number of GO terms with a p -value < 0.05 varied among both hosts and at the different stages. A complete list of GO terms for both hosts at the studied stage is shown in S3 Table.

Through GO enrichment analysis, we identified specific GO terms within the differentially expressed genes associated with the parasitic plant-host interaction, as previously reported in the literature [55–61]. In the susceptible host (S_Host), we observed the enrichment of GO terms related to secondary metabolites, particularly flavonoids in the up-regulated gene set at the AG stage (Fig 4B). However, we did not detect significant enrichment of GO terms in the down-regulated gene set at the BG stage in the S_Host transcriptome (S3 Table). Conversely, in the resistant host (R_Host), we identified several significantly enriched GO terms among the differentially expressed genes. Firstly, in the R_Host at the BG stage, we observed the enrichment of GO terms associated with flavonoid pathways including "flavonoid biosynthetic process" (GO:0009813) in the down-regulated gene set. At the AG stage, both "flavonoid biosynthetic process" (GO:0009813) and "flavonoid metabolic process" (GO:0009812) GO terms were enriched in the up-regulated gene set (S3 Table).

Secondly, in the R_Host at the BG stage, we identified the enrichment of GO terms related to auxin pathways in the down-regulated gene set, including "regulation of auxin-mediated signaling pathway" (GO:0010928), "auxin polar transport" (GO:0009926), "auxin transport" (GO:0060918), and "auxin efflux" (GO:0010315) (Fig 5D, S3 Table). Moreover, in the up-regulated gene set at the BG stage in the R_Host, Thiamine GO terms as well as "actin filament-based transport" (GO:0099515) (Fig 5A) and "actin filament-based movement" (GO:0030048) GO terms were enriched (S3 Table).

Regarding the jasmonic acid pathways, differences were observed among the studied stages. At the BG stage in the R_Host, "jasmonic acid metabolic process" (GO:0009694) was enriched in the down-regulated gene set. At the AG stage, in the R_Host, "jasmonic acid-mediated signaling pathway" (GO:0009867), "response to jasmonic acid" (GO:0009753), "jasmonic acid biosynthetic process" (GO:0009695), and "regulation of jasmonic acid-mediated signaling pathway" (GO:2000022) were enriched in the up-regulated gene set. However, at this same stage in the S_Host, "response to jasmonic acid" (GO:0009753) was identified among the up-regulated gene set but with an insignificant p -value (S3 Table).

Marker genes. To enhance our understanding of molecular distinctions between the susceptible and resistant hosts in response to *O. foetida* attack, we focused on the gene expression profiles of the WRKY family and the orobanchol biosynthesis pathway. This strategic choice is driven by critical role of germination stimulants, particularly orobanchol, in *Orobanche* spp.

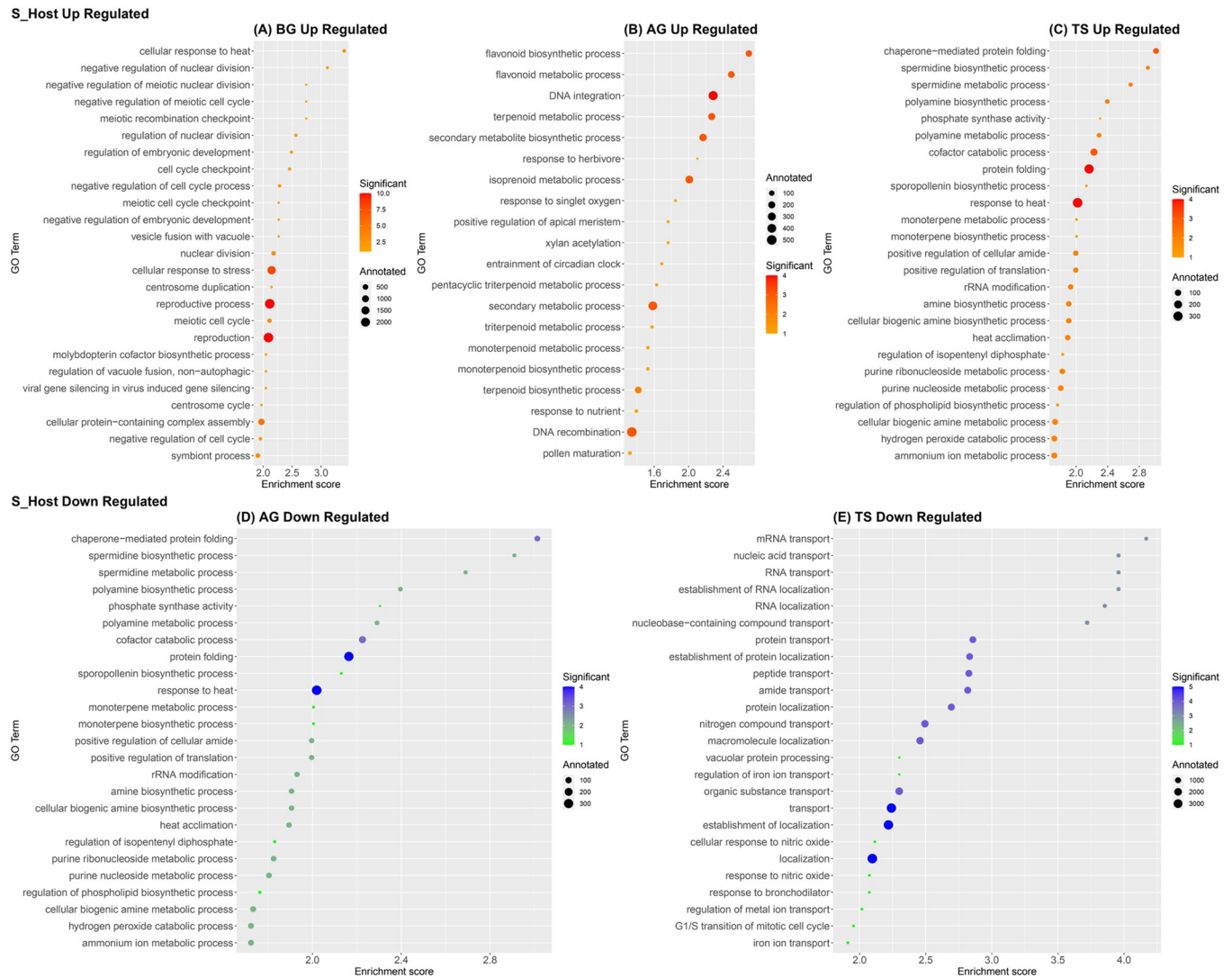


Fig 4. A bubble plot displaying the top 25 of significant enriched gene ontology (GO) terms of differentially expressed genes (DEGs), in the susceptible *Vicia faba* host (S_Host) during *Orobanche foetida* attack. GO terms enriched within the up-regulated gene set at the Before Germination (BG) stage (A), at the After Germination (AG) stage (B) and at the Tubercle Stage (TS) stage (C). GO terms enriched within the down-regulated gene set at the After Germination (AG) stage (D) and at the Tubercle Stage (TS) stage (E). Bubble sizes represent the total number of genes in *Vicia faba* genome with a given GO term “Annotated”. Bubble colors indicate the number of genes observed to be significantly differentially expressed “Significant”. The enrichment score represents “-log10(elimFisher)”.

<https://doi.org/10.1371/journal.pone.0301981.g004>

seed germination, and the known involvement of certain WRKY genes in responses to parasitic plants, as previously revealed in sunflower in response to *O. cumana* attack [50]. To visualize the expression patterns of target transcripts at BG, AG, and TS stages for both susceptible (S_Host) and resistant (R_Host) hosts, at gene count level, we employed box plots (Figs 6 and 7). The unigenes generated by the Corset software served as the basis for both analyses.

Among the 20 target AtWRKY proteins (S1 Table), we detected expression in 13 genes. Notably, it is essential to clarify that our BLASTx analysis considered more than one isoform for these proteins. According to Fig 6, we distinguished the absence of expression of AtWRKY46 homolog in R_Host at the three studied stages. Similarly, we didn't detect the expression of the homolog of the second isoform of AtWARKY1 in the S_Host. Whereas the

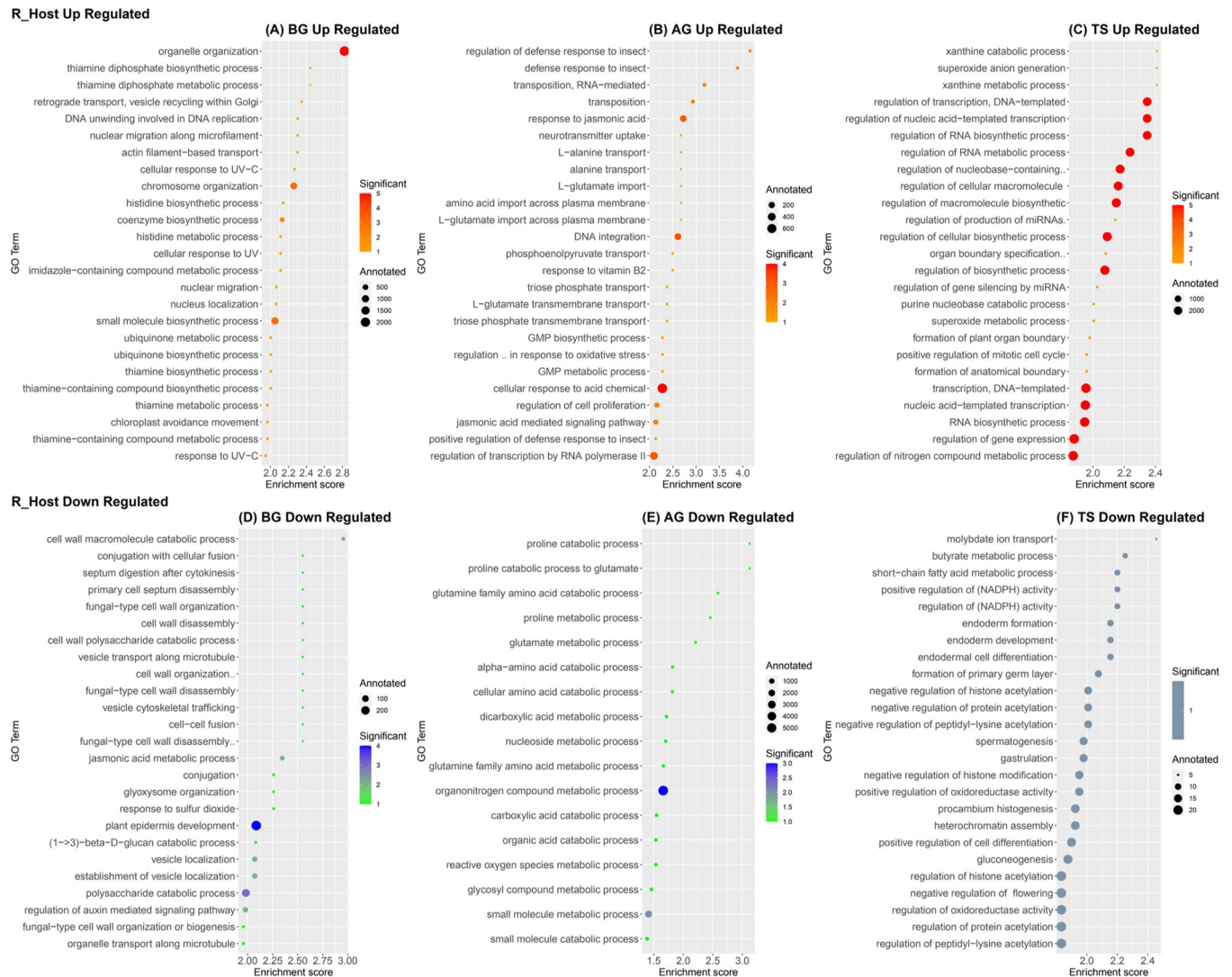


Fig 5. A bubble plot displaying the top 25 of significant enriched gene ontology (GO) terms of differentially expressed genes (DEGs), in the resistant *Vicia faba* host (R_Host) during *Orobancha foetida* attack. GO terms enriched within the up-regulated gene set at the Before Germination (BG) stage (A), at the After Germination (AG) stage (B) and at the Tubercle Stage (TS) stage (C). GO terms enriched within the down-regulated gene set at the Before Germination (BG) stage. (E) Significant down-regulated GO terms at the After Germination (AG) stage. (F) Significant down-regulated GO terms at the Tubercle Stage (TS) stage. Bubble sizes represent the total number of genes in *Vicia faba* genome with a given GO term “Annotated”. Bubble colors indicate the number of genes observed to be significantly differentially expressed “Significant”. The enrichment score represents “-log₁₀(elimFisher)”.

<https://doi.org/10.1371/journal.pone.0301981.g005>

first isoform of AtWARKY1 and AtWRKY30 were detected only at the TS stage in the R_Host. The first isoform of AtWRKY18 was only expressed at the AG stage in the R_Host. Regarding AtWRKY4, we didn’t detect the expression of the first isoform in the S_Host at all stages, while expression occurs of the second isoform at the AG stage. However, both isoforms were expressed in the R_Host at the three studied stages. AtWARKY71 was not detected at the TS stage in the R_Host and at the AG stage in the S_Host. Moreover, the homologs of AtWRKY3, AtWRKY6, AtWRKY22, AtWRKY33, AtWRKY40, AtWRKY53, AtWRKY70 were expressed in both hosts at the three stages with slight differences.

Regarding the orobanchol biosynthesis pathway (Fig 7A), we detected the expression of all the homologs except the D27. Indeed, the Blastx analysis revealed a hit for the D27 homolog

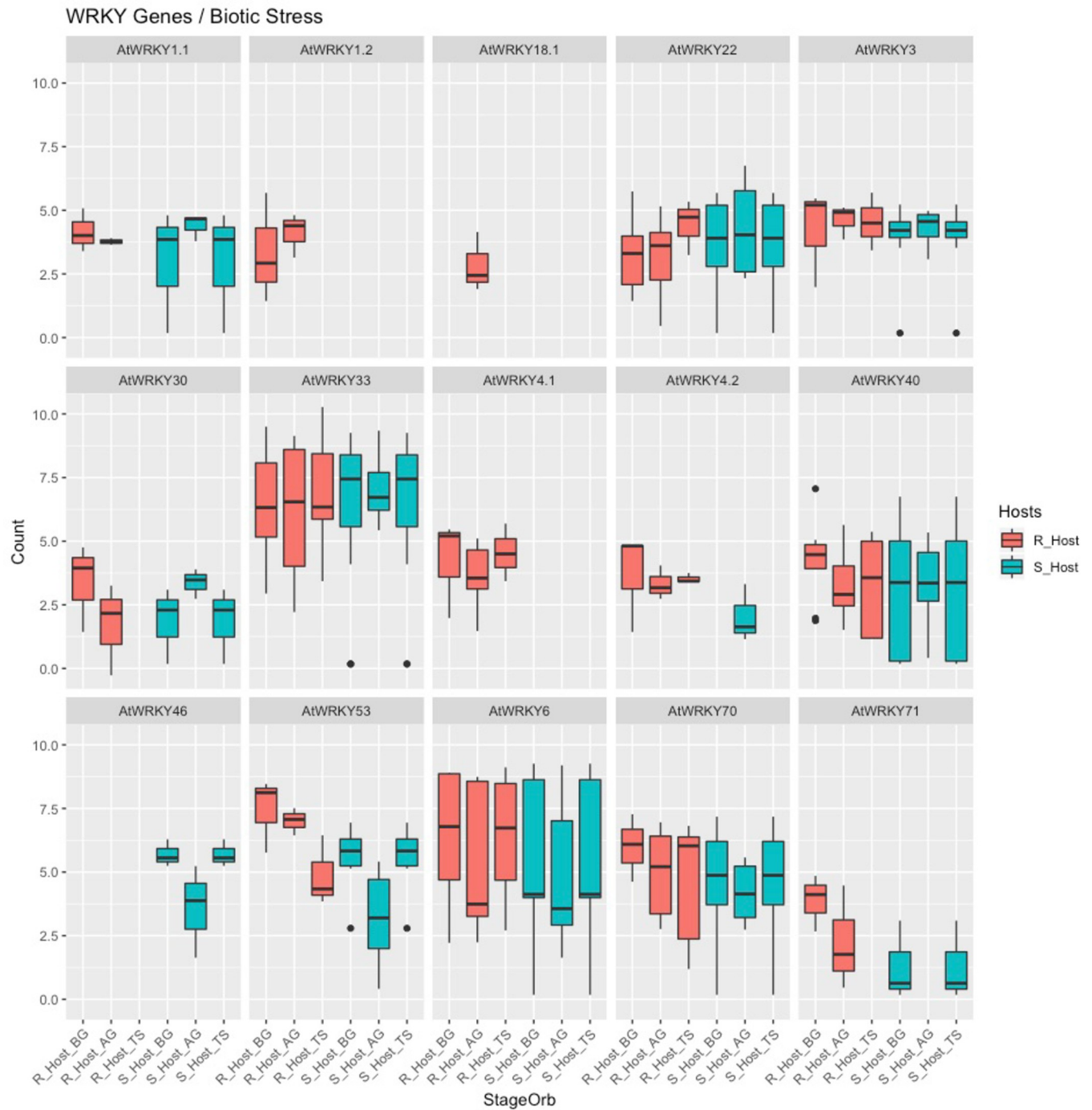


Fig 6. Box plots displaying the TMM-normalized count (Count) of AtWRKY genes homologs in two *Vicia faba* varieties: A susceptible (S_Host) and a resistant (R_Host) against *Oranbanche foetida* attack at the three studied stages (StageOrb); Before Germination (BG), After Germination (AG) and Tubercle Stage (TS).

<https://doi.org/10.1371/journal.pone.0301981.g006>

but the expression was so low to be detected. The AtCDD7 homolog was expressed in both hosts at the same stage (AG), while the AtCDD8 homolog was expressed in both hosts at all the stages (Fig 7B). Regarding the MAX1, belonging to the CYP11A subfamily, we studied the expression of two isoforms from *Arabidopsis thaliana* and two from *Medicago truncatula*.

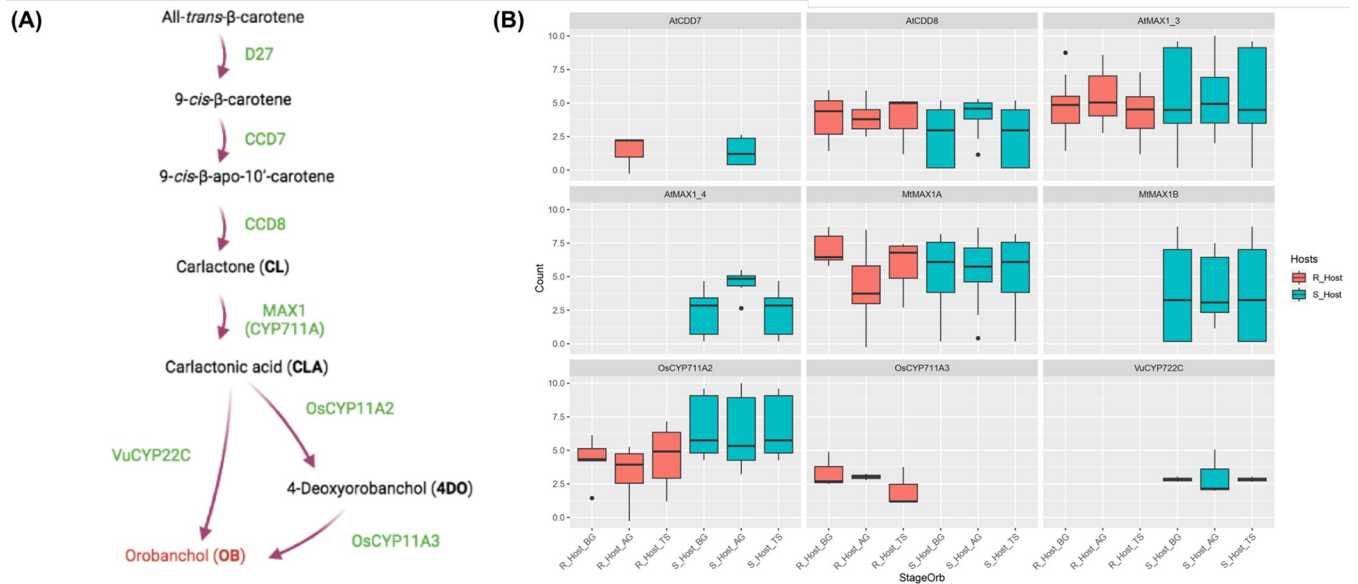


Fig 7. (A) Orobanchol biosynthesis pathway [50]. (B) Box plots displaying the TMM-normalized count of orobanchol Biosynthesis genes homologs in two *Vicia faba* varieties. A susceptible (S_Host) and a resistant (R_Host) against *Orobancha foetida* attack at the three studied stages; Before Germination (BG), After Germination (AG) and Tubercle Stage (TS).

<https://doi.org/10.1371/journal.pone.0301981.g007>

Moreover, AtMAX1_4 and MtMAX1B homologs were only expressed in the S_Host at all the stages. AtMAX1_3 and MtMAX1A homologs were expressed in both hosts (Fig 7B). Furthermore, the OsCYP711A2 homolog expression was slightly higher in the S_Host than in the R_Host at the three studied stages. Additionally, the OsCYP711A3 homolog was only expressed in the R_Host. Whereas, the VuCYP722C homolog was only expressed in the S_Host (Fig 7B). For more understanding of this pattern, we tested the presence of the non-expressed genes involved in orobanchol biosynthesis pathway in both *V. faba* varieties' used in this study as resistant and susceptible hosts. Our results showed the presence of all the studied homolog genes (AtMAX1, MtMAX1B, VuCYP722C and OsCYP711A3) in both host plant genomes, indicating that differences occur at the gene expression level.

Discussion

In the present study, we investigated the gene expression of two faba bean varieties (*V. faba minor*) (resistant and susceptible) during the *O. foetida* attack at root level using RNAseq. To the best of our knowledge, this is the first study showing the global changes in gene expression taking place in hosts in response to *O. foetida* parasitism. In this work, we studied the pre-attachment resistance displayed by the absence of *O. foetida* seed germination in the presence of the R_Host.

Prior to functional annotation analysis, we observed differences between the hosts transcriptomes in terms of number of contigs and the number of differentially expressed genes (DEGs). Indeed, we counted a greater number of contigs and DEGs in the S_Host assembly compared to the R_Host assembly. This differences between the studied hosts could be attributed to differences in sequencing depth (number of pooled reads; S_Host = 33,442,981; R_Host = 27,641,999).

To gain an insight into the biological functions of the differentially expressed genes, we performed a GO enrichment analysis at the three studied stages (BG, AG, TS). Therefore, differences in response to *O. foetida* attack arises. Indeed, in the susceptible host (S_Host), we

detected the GO terms related to secondary metabolites such as flavonoids at the AG stage in the up-regulated gene set. In fact, host-derived secondary metabolites are involved in the plant–parasite interaction after germination [56], and data from the literature suggests that flavonoids promote haustoria formation in the root parasite *Triphysaria versicolor* [55]. Regarding the resistant host (R_Host), we detected the Thiamine GO terms during the BG stage in the up-regulated gene set. The thiamine plays a role as a response molecule towards abiotic and biotic stresses suggesting that boosting thiamine content could increase resistance to stresses [59]. Nevertheless, other study showed that plants with higher accumulation of thiamin did not show enhanced resistance to the bacteria *Xanthomonas oryzae* [62]. Furthermore, we detected the auxin GO terms at the BG stage in the R_Host in the down-regulated gene set. This phytohormone was reported to be involved in host-parasitic plant interaction by controlling xylem vessel connections between parasite and host [58]. The actin filament-based transport and movement GO terms were also detected at the BG stage in the R_Host in the up-regulated gene set. In fact, the cytoskeleton may play an extremely complex role in plant immunity via the reorganization of the actin cytoskeleton [61]. Additionally, we detected the GO term “jasmonic acid mediated signaling pathway” at the AG in the R_Host in the up-regulated gene set. Whereas, a response to jasmonic acid Go Term (GO:0009753) was detected in S_Host at the AG stage but with an insignificant *p*-value in the up-regulated gene set. In addition, the transcriptomic analysis of *H. annuus* roots resistance to *O. cumana* showed that the expression of the Jasmonate ZIM-domain (JAZ) proteins, which act as inhibitory factors of the jasmonic acid (JA), was higher in the resistant sunflower host than in the susceptible host [60]. In fact, variations in the response to parasitic plant attacks were reported. For instance, it has been revealed that a moderately resistant sorghum cultivar appears to recognize *Striga* parasitism as both wounding and microbial stress by inducing SA and JA-responsive genes in the root [63]. However, the *Striga* parasitism induces JA-responsive genes and suppress SA-responsive genes in the roots of highly susceptible cultivars, suggesting that susceptible hosts recognize *Striga* parasitism as wounding stress rather than microbial stress. Whereas, *H. annuus* /*O. cumana* interaction the upregulation of SA-responsive genes were detected [42].

Moreover, prior studies have noted the importance of the WRKYs genes in plant immune responses to various biotic stresses. In fact, this genes' family has been found to be involved in the microbe-associated molecular pattern-triggered immunity, PAMP-triggered immunity or effector-triggered immunity, or system acquired resistance [64]. Interestingly, this genes family were previously reported to be involved in *H. annuus*/*O. cumana* interaction. Thus, we decided to explore WRKYs genes expression in faba bean under attack of *O. foetida*. We detected the expression of the AtWRKY46 homolog only in the S_Host at the three studied stages. This gene is probably involved in the SA signaling pathway [65]. During the *H. annuus*/*O. cumana*, WRKY genes (HaWRKY7/15/44/45/68/71/72/76/85) were induced in sunflower resistant cultivar and repressed in susceptible cultivar during *H. annuus*/*O. cumana* interaction [66]. This finding suggests a potential role of these WRKYs genes in conferring resistance to sunflower against *O. cumana* [67]. Nevertheless, in our study we didn't observe this kind of pattern which highlights the need to characterize some WRKY genes as specifically involved in *V. faba*/*O. foetida* interaction.

In the present work, we did not detect any similar pattern to those cited above. This could be explained by the nature of the resistance. In fact, in our study we detect a pre-attachment resistance and not post-attachment resistance. Therefore, we decided to explore the expression of genes involved in the orobanchol biosynthesis pathway. SL biosynthesis (Fig 7A) begins with DWARF 27 (D27) catalysis of isomerization of the C9-C10 double bond in all-trans- β -carotene, followed by carotenoid cleavage dioxygenase 7 (CCD7) and CCD8 catalysis of sequential carotenoid cleavage reactions to form a biosynthetic intermediate, carlactone (CL)

[51]. The carlactone (CL) is then converted to carlactonic acid (CLA) by cytochrome P450 monooxygenase (CYP); in *A. thaliana* AtCYP711A1 encoded by MORE AXIALLY GROWTH 1 (AtMAX1), and in *Oryza sativa* by OsCYP711As [68,69]. To produce orobanchol, two possible biosynthesis pathways were identified. Firstly, an indirect pathway observed in rice, OsCYP711A2/Os900 catalyzes the conversion of CLA to 4-deoxyorobanchol (4DO), which is converted to Orobanchol by OsCYP711A3/Os1400 [51]. Secondly, a direct pathway by the conversion of CLA to orobanchol by CYP722C as demonstrated in cowpea (VuCYP722C) and tomato (SlCYP722C) [70] (Fig 7A).

In the present study, at gene count level, we detected differences between the studied *V. faba* varieties (S_Host and R_Host) of genes homologs involved in orobanchol biosynthesis downstream of CLA. Within the S_Host, we detect the expression of AtMAX1, MtMAX1B and VuCYP722C homologs but not OsCYP711A3. However, in the R_Host we detected the expression of CYP711A3 homolog. In this context, the rice cultivar Bara which is deficient in CYP711A3/Os1400 retains the ability to produce orobanchol [69]. Moreover, the catalyzing property of CL and CLA of CYP711A subfamily to canonical SLs in seed plant was exclusively detected only in rice [71]. In a previous study on faba bean, a genitor of our R_Host was used as a resistant host, and orobanchol was not detected in its root exudates [72]. Whereas, orobanchol and orobanchol acetate were detected in the root exudates of the same S_Host variety used in our study [72]. This accords with other studies, which showed that orobanchol producing plants (cowpea, red clover, pea, red bell pepper) convert CLA to orobanchol but did not convert exogenously administered 4DO to orobanchol [73,74].

All the studied homologs genes involved in the orobanchol biosynthesis pathway are present in both hosts (S_Host and R_Host) in this study (AtMAX1, MtMAX1B, VuCYP722C and OsCYP711A3). However, we detected differences in gene expression between the susceptible and the resistant hosts, particularly, concerning the VuCYP722C homolog, coding for a key enzyme involved in orobanchol biosynthesis. Interestingly, this gene was successfully knocked out using the CRISPR technique, effectively inhibiting orobanchol production in tomato roots [70]. Therefore, it can be assumed that targeting this gene in order to develop resistant varieties is a promising outcome. With this in prospect, it would be recommendable to characterize faba bean genes involved in orobanchol biosynthesis pathway. Additionally, it will be interesting to conduct histological study in order to describe and characterize key time points during *V. faba*/*O. foetida* interaction as already shown for *Striga* [75]. This kind of study will allow to target more efficiently molecular changes during this interaction.

Supporting information

S1 Table. A list of WRKYs proteins involved in plant defense during a biotic stress.

(XLSX)

S2 Table. A list of proteins involved in orobanchol biosynthesis pathway.

(XLSX)

S3 Table. A complete list of differential expressed GO terms (biological process).

(XLSX)

Author Contributions

Conceptualization: Amal Boukteb, Mariem Bouhadida.

Data curation: Amal Boukteb, Kazuki Sato, Pamela Gan, Yasunori Ichihashi.

Formal analysis: Amal Boukteb, Kazuki Sato, Pamela Gan, Yasunori Ichihashi.

Funding acquisition: Amal Boukteb, Mohamed Kharrat, Ken Shirasu, Mariem Bouhadida.

Investigation: Amal Boukteb, Hanen Sakouhi, Arisa Shibata, Mariem Bouhadida.

Methodology: Amal Boukteb, Kazuki Sato, Pamela Gan, Yasunori Ichihashi.

Project administration: Yasunori Ichihashi, Mariem Bouhadida.

Resources: Amal Boukteb, Mohamed Kharrat, Ken Shirasu, Mariem Bouhadida.

Supervision: Yasunori Ichihashi, Mariem Bouhadida.

Validation: Amal Boukteb, Yasunori Ichihashi, Mariem Bouhadida.

Visualization: Amal Boukteb.

Writing – original draft: Amal Boukteb, Yasunori Ichihashi, Mariem Bouhadida.

Writing – review & editing: Amal Boukteb, Yasunori Ichihashi, Mariem Bouhadida.

References

1. Tanno K, Willcox G. The origins of cultivation of *Cicer arietinum* L. and *Vicia faba* L.: early finds from Tell el-Kerkh, north-west Syria, late 10th millennium B.P. *Veg Hist Archaeobotany*. 2006; 15: 197–204.
2. Caracuta V, Weinstein-Evron M, Kaufman D, Yeshurun R, Silvent J, Boaretto E. 14,000-year-old seeds indicate the Levantine origin of the lost progenitor of faba bean. *Sci Rep*. 2016; 6: 37399. <https://doi.org/10.1038/srep37399> PMID: 27876767
3. Pérez-de-Luque A, Eizenberg H, Grenz JH, Sillero JC, Ávila C, Sauerborn J, et al. Broomrape management in faba bean. *Field Crops Res*. 2010; 115: 319–328. <https://doi.org/10.1016/j.fcr.2009.02.013>
4. FAOSTAT. Food and Agriculture Organization of the United Nations Statistics. <https://www.fao.org/faostat/en/#data/QCL>. Accessed 28 March 2023. 2021.
5. Herridge DF, Peoples MB, Boddey RM. Global inputs of biological nitrogen fixation in agricultural systems. *Plant Soil*. 2008; 311: 1–18. <https://doi.org/10.1007/s11104-008-9668-3>
6. Aschi A, Aubert M, Riah-Anglet W, Nélieu S, Dubois C, Akpa-Vinceslas M, et al. Introduction of Faba bean in crop rotation: Impacts on soil chemical and biological characteristics. *Appl Soil Ecol*. 2017; 120: 219–228. <https://doi.org/10.1016/j.apsoil.2017.08.003>
7. Dubova L, Alsiņa I, Ruža A, Šenberga A. Impact of faba bean (*Vicia faba* L.) cultivation on soil microbiological activity. 2018; 2016–2025. <https://doi.org/10.15159/ar.18.195>
8. Mouradi M, Farissi M, Makoudi B, Bouizgaren A, Ghoulam C. Effect of faba bean (*Vicia faba* L.)–rhizobia symbiosis on barley's growth, phosphorus uptake and acid phosphatase activity in the intercropping system. *Ann Agrar Sci*. 2018; 16: 297–303. <https://doi.org/10.1016/j.aasci.2018.05.003>
9. Xiao J, Yin X, Ren J, Zhang M, Tang L, Zheng Y. Complementation drives higher growth rate and yield of wheat and saves nitrogen fertilizer in wheat and faba bean intercropping. *Field Crops Res*. 2018; 221: 119–129. <https://doi.org/10.1016/j.fcr.2017.12.009>
10. Xu Y, Qiu W, Sun J, Müller C, Lei B. Effects of wheat/faba bean intercropping on soil nitrogen transformation processes. *J Soils Sediments*. 2019; 19: 1724–1734. <https://doi.org/10.1007/s11368-018-2164-3>
11. Martineau-Côté D, Achouri A, Karboune S, L'Hocine L. Faba Bean: An Untapped Source of Quality Plant Proteins and Bioactives. *Nutrients*. 2022; 14: 1541. <https://doi.org/10.3390/nu14081541> PMID: 35458103
12. DGPA. Direction Générale de la Production Agricole en Tunisie. 2021.
13. Kharrat M. Étude sur le Secteur des Légumineuses Alimentaires et Fourragères en Tunisie. Tunis, Tunisia: FAO; 2021.
14. Abbes Z, Kharrat M, de Tunisie, Karray RH, Chaïbi W. Seed Germination and Tubercle Development of *Orobanche foetida* and *Orobanche crenata* in Presence of Different Plant Species. 2008; 3: 11.
15. Delavault P, Montiel G, Brun G, Pouvreau J-B, Thoiron S, Simier P. Chapter Three—Communication Between Host Plants and Parasitic Plants. In: Becard G, editor. *Advances in Botanical Research*. Academic Press; 2017. pp. 55–82. <https://doi.org/10.1016/bs.abr.2016.10.006>
16. Abbes Z, Kharrat M, Delavault P, Simier P, Chaïbi W. Field evaluation of the resistance of some faba bean (*Vicia faba* L.) genotypes to the parasitic weed *Orobanche foetida* Poir. *Crop Prot*. 2007; 26: 1777–1784. <https://doi.org/10.1016/j.cropro.2007.03.012>

17. Amri M, Trabelsi I, Abbes Z, Kharrat M. Release of a New Faba Bean Variety “Chourouk” Resistant to the Parasitic Plants *Orobanche foetida* and *Orobanche crenata* in Tunisia. 2019; 21: 7.
18. Amri M, Abbes Z, Trabelsi I, Ghanem ME, Mentag R, Kharrat M. Chlorophyll content and fluorescence as physiological parameters for monitoring *Orobanche foetida* Poir. infection in faba bean. PLOS ONE. 2021; 16: e0241527. <https://doi.org/10.1371/journal.pone.0241527> PMID: 34032807
19. Boeuf F. Les Orobanches en Tunisie. J Agriculture Prat. 1905; 9: 11–14. Available: www.gallica.fr.
20. Chabrolin CH. Contribution à l'étude de la germination des graines de l'Orobanche de la fève. Annales du service botanique et agronomique de la direction des affaires économiques de Tunisie. 1939: 91–145.
21. Kharrat M, Halila MH, Linke KH, Haddar T. First report of *Orobanche foetida* Poir on faba bean in Tunisia. Fabis Newsletter 30. 1992: 46–47.
22. Poir L. Voyage en Barbarie, ou lettres écrites de l'ancienne numide. Library of the New York Botanical Garden; 1922.
23. Román B, Alfaro C, Torres AM, Moreno MT, Satovic Z, Pujadas A, et al. Genetic Relationships among *Orobanche* Species as Revealed by RAPD Analysis. Ann Bot. 2003; 91: 637–642. <https://doi.org/10.1093/aob/mcg060> PMID: 12714362
24. Schneeweiss GM, Colwell A, Park J-M, Jang C-G, Stuessy TF. Phylogeny of holoparasitic *Orobanche* (*Orobanchaceae*) inferred from nuclear ITS sequences. Mol Phylogenet Evol. 2004; 30: 465–478. [https://doi.org/10.1016/S1055-7903\(03\)00210-0](https://doi.org/10.1016/S1055-7903(03)00210-0) PMID: 14715236
25. Kharrat M. Étude de la virulence de l'écotype de Béja d' *Orobanche foetida* sur différentes espèces de légumineuses. GTZ Tunis, Tunisia; 2002. p. 89.
26. Amri M, Sellami F, Kharrat M, Karray RH. First Report of the Parasitic Plant *Orobanche foetida* on Fenu-greek (*Trigonella foenum-graecum*) in Tunisia. 2009; 4: 4.
27. Boukteb A, Sakaguchi S, Ichihashi Y, Kharrat M, Nagano AJ, Shirasu K, et al. Analysis of Genetic Diversity and Population Structure of *Orobanche foetida* Populations From Tunisia Using RADseq. Front Plant Sci. 2021; 12. <https://doi.org/10.3389/fpls.2021.618245> PMID: 33927733
28. Kharrat M, Halila MH. *Orobanche* species on faba bean (*Vicia faba* L.) in Tunisia: problem and management. Amsterdam, Netherlands; 1994.
29. Rubiales D, Sadiki M, Román B. First Report of *Orobanche foetida* on Common Vetch (*Vicia sativa*) in Morocco. Plant Dis. 2005; 89: 528–528. <https://doi.org/10.1094/PD-89-0528A> PMID: 30795439
30. Román B, Hernandez R, Pujadas-Salva AJ, Cubero JI, Rubiales D, Satovic Z. Genetic diversity in two variants of *Orobanche gracilis* Sm. [var. *gracilis* and var. *deludens* (Beck) A. Pujadas] (*Orobanchaceae*) from different regions of Spain. Electron J Biotechnol. 2007; 10: 221–229. <https://doi.org/10.2225/vol10-issue2-fulltext-6>
31. Vaz Patto MC, Díaz-Ruiz R, Satovic Z, Román B, Pujadas-Salva AJ, Rubiales D. Genetic diversity of Moroccan populations of *Orobanche foetida*: evolving from parasitising wild hosts to crop plants. Weed Res. 2008; 48: 179–186. <https://doi.org/10.1111/j.1365-3180.2008.00621.x>
32. Cook CE, Whichard LP, Turner B, Wall ME, Eglely GH. Germination of Witchweed (*Striga lutea* Lour.): Isolation and Properties of a Potent Stimulant. Science. 1966; 154: 1189–1190. <https://doi.org/10.1126/science.154.3753.1189> PMID: 17780042
33. Yokota T, Sakai H, Okuno K, Yoneyama K, Takeuchi Y. Alectrol and orobanchol, germination stimulants for *Orobanche minor*, from its host red clover. Phytochemistry. 1998; 49: 1967–1973. [https://doi.org/10.1016/S0031-9422\(98\)00419-1](https://doi.org/10.1016/S0031-9422(98)00419-1)
34. Yoneyama K, Brewer PB. Strigolactones, how are they synthesized to regulate plant growth and development? Curr Opin Plant Biol. 2021; 63: 102072. <https://doi.org/10.1016/j.pbi.2021.102072> PMID: 34198192
35. Yoshida S, Cui S, Ichihashi Y, Shirasu K. The Haustorium, a Specialized Invasive Organ in Parasitic Plants. Annu Rev Plant Biol. 2016; 67: 643–667. <https://doi.org/10.1146/annurev-arplant-043015-111702> PMID: 27128469
36. Draie R, Péron T, Pouvreau J-B, Véronési C, Jégou S, Delavault P, et al. Invertases involved in the development of the parasitic plant *Phelipanche ramosa*: characterization of the dominant soluble acid isoform, PrSA11. Mol Plant Pathol. 2011; 12: 638–652. <https://doi.org/10.1111/j.1364-3703.2010.00702.x> PMID: 21726369
37. Labrousse P, Arnaud MC, Serieys H, Bervillé A, Thalouarn P. Several Mechanisms are Involved in Resistance of Helianthus to *Orobanche cumana* Wallr. Ann Bot. 2001; 88: 859–868. <https://doi.org/10.1006/anbo.2001.1520>
38. Swarbrick PJ, Huang K, Liu G, Slate J, Press MC, Scholes JD. Global patterns of gene expression in rice cultivars undergoing a susceptible or resistant interaction with the parasitic plant *Striga*

- hermonthica. *New Phytol.* 2008; 179: 515–529. <https://doi.org/10.1111/j.1469-8137.2008.02484.x> PMID: 19086183
39. Mutuku JM, Yoshida S, Shimizu T, Ichihashi Y, Wakatake T, Takahashi A, et al. The WRKY45-Dependent Signaling Pathway Is Required For Resistance against *Striga hermonthica* Parasitism. *Plant Physiol.* 2015; 168: 1152–1163. <https://doi.org/10.1104/pp.114.256404> PMID: 26025049
 40. Saucet SB, Shirasu K. Molecular Parasitic Plant–Host Interactions. *PLOS Pathog.* 2016; 12: e1005978. <https://doi.org/10.1371/journal.ppat.1005978> PMID: 27977782
 41. de Zélicourt A, Letousey P, Thoiron S, Campion C, Simoneau P, Elmorjani K, et al. Ha-DEF1, a sunflower defensin, induces cell death in *Orobanchae* parasitic plants. *Planta.* 2007; 226: 591–600. <https://doi.org/10.1007/s00425-007-0507-1> PMID: 17375322
 42. Letousey P, De Zélicourt A, Vieira Dos Santos C, Thoiron S, Monteau F, Simier P, et al. Molecular analysis of resistance mechanisms to *Orobanchae cumana* in sunflower. *Plant Pathol.* 2007; 56: 536–546. <https://doi.org/10.1111/j.1365-3059.2007.01575.x>
 43. Ichihashi Y, Kusano M, Kobayashi M, Suetsugu K, Yoshida S, Wakatake T, et al. Transcriptomic and Metabolomic Reprogramming from Roots to Haustoria in the Parasitic Plant, *Thesium chinense*. *Plant Cell Physiol.* 2018; 59: 729–738. <https://doi.org/10.1093/pcp/pcx200> PMID: 29281058
 44. Grabherr MG, Haas BJ, Yassour M, Levin JZ, Thompson DA, Amit I, et al. Trinity: reconstructing a full-length transcriptome without a genome from RNA-Seq data. *Nat Biotechnol.* 2011; 29: 644–652. <https://doi.org/10.1038/nbt.1883>
 45. Nishimura O, Hara Y, Kuraku S. gVolante for standardizing completeness assessment of genome and transcriptome assemblies. *Bioinforma Oxf Engl.* 2017; 33: 3635–3637. <https://doi.org/10.1093/bioinformatics/btx445> PMID: 29036533
 46. Simão FA, Waterhouse RM, Ioannidis P, Kriventseva EV, Zdobnov EM. BUSCO: assessing genome assembly and annotation completeness with single-copy orthologs. *Bioinformatics.* 2015; 31: 3210–3212. <https://doi.org/10.1093/bioinformatics/btv351> PMID: 26059717
 47. Langmead B, Salzberg SL. Fast gapped-read alignment with Bowtie 2. *Nat Methods.* 2012; 9: 357–359. <https://doi.org/10.1038/nmeth.1923> PMID: 22388286
 48. Davidson NM, Oshlack A. Corset: enabling differential gene expression analysis for de novo assembled transcriptomes. *Genome Biol.* 2014; 15: 410. <https://doi.org/10.1186/s13059-014-0410-6> PMID: 25063469
 49. Risso D, Ngai J, Speed TP, Dudoit S. Normalization of RNA-seq data using factor analysis of control genes or samples. *Nat Biotechnol.* 2014; 32: 896–902. <https://doi.org/10.1038/nbt.2931> PMID: 25150836
 50. Wani SH, Anand S, Singh B, Bohra A, Joshi R. WRKY transcription factors and plant defense responses: latest discoveries and future prospects. *Plant Cell Rep.* 2021; 40: 1071–1085. <https://doi.org/10.1007/s00299-021-02691-8> PMID: 33860345
 51. Wakabayashi T, Ueno K, Sugimoto Y. Structure Elucidation and Biosynthesis of Orobanchol. *Front Plant Sci.* 2022; 13. <https://doi.org/10.3389/fpls.2022.835160> PMID: 35222492
 52. Adrian A, Jorg R. topGO: Enrichment Analysis for Gene Ontology. 2018.
 53. Emms DM, Kelly S. OrthoFinder: phylogenetic orthology inference for comparative genomics. *Genome Biol.* 2019; 20: 238. <https://doi.org/10.1186/s13059-019-1832-y> PMID: 31727128
 54. Saghai-Maroo MA, Soliman KM, Jorgensen RA, Allard RW. Ribosomal DNA spacer-length polymorphisms in barley: mendelian inheritance, chromosomal location, and population dynamics. *Proc Natl Acad Sci U S A.* 1984; 81: 8014–8018. <https://doi.org/10.1073/pnas.81.24.8014> PMID: 6096873
 55. Albrecht H, Yoder JI, Phillips DA. Flavonoids promote haustoria formation in the root parasite *triphysaria versicolor*. *Plant Physiol.* 1999; 119: 585–592. <https://doi.org/10.1104/pp.119.2.585> PMID: 9952454
 56. Bouwmeester HJ, Matusova R, Zhongkui S, Beale MH. Secondary metabolite signalling in host–parasitic plant interactions. *Curr Opin Plant Biol.* 2003; 6: 358–364. [https://doi.org/10.1016/s1369-5266\(03\)00065-7](https://doi.org/10.1016/s1369-5266(03)00065-7) PMID: 12873531
 57. Hiraoka Y, Sugimoto Y. Molecular Responses of Sorghum to Purple Witchweed (*Striga hermonthica*) Parasitism. *Weed Sci.* 2008; 56: 356–363. <https://doi.org/10.1614/WS-07-136.1>
 58. Ishida JK, Wakatake T, Yoshida S, Takebayashi Y, Kasahara H, Wafula E, et al. Local Auxin Biosynthesis Mediated by a YUCCA Flavin Monooxygenase Regulates Haustorium Development in the Parasitic Plant *Phtheirospermum japonicum*. *Plant Cell.* 2016; 28: 1795–1814. <https://doi.org/10.1105/tpc.16.00310> PMID: 27385817
 59. Subki A, Abidin AAZ, Yusof ZNB. The Role of Thiamine in Plants and Current Perspectives in Crop Improvement. LeBlanc JG, Giori GS de, editors. 2018; 33–44. <https://doi.org/10.5772/intechopen.79350>

60. Zhang Y, Su J, Yun X, Wu W, Wei S, Huang Z, et al. Molecular mechanism of the parasitic interaction between *Orobancha cumana* wallr. and sunflowers. *J Plant Interact.* 2022; 17: 549–561. <https://doi.org/10.1080/17429145.2022.2062061>
61. Wang J, Lian N, Zhang Y, Man Y, Chen L, Yang H, et al. The Cytoskeleton in Plant Immunity: Dynamics, Regulation, and Function. *Int J Mol Sci.* 2022; 23: 15553. <https://doi.org/10.3390/ijms232415553> PMID: 36555194
62. Dong W, Thomas N, Ronald PC, Goyer A. Overexpression of Thiamin Biosynthesis Genes in Rice Increases Leaf and Unpolished Grain Thiamin Content But Not Resistance to *Xanthomonas oryzae* pv. *oryzae*. *Front Plant Sci.* 2016; 7.
63. Timko MP, Scholes JD. Host Reaction to Attack by Root Parasitic Plants. In: Joel DM, Gressel J, Muselman LJ, editors. *Parasitic Orobanchaceae: Parasitic Mechanisms and Control Strategies.* Berlin, Heidelberg: Springer; 2013. pp. 115–141. https://doi.org/10.1007/978-3-642-38146-1_7
64. Chen F, Hu Y, Vannozzi A, Wu K, Cai H, Qin Y, et al. The WRKY Transcription Factor Family in Model Plants and Crops. *Crit Rev Plant Sci.* 2017; 36: 311–335. <https://doi.org/10.1080/07352689.2018.1441103>
65. Hu Y, Dong Q, Yu D. *Arabidopsis* WRKY46 coordinates with WRKY70 and WRKY53 in basal resistance against pathogen *Pseudomonas syringae*. *Plant Sci.* 2012; 185–186: 288–297. <https://doi.org/10.1016/j.plantsci.2011.12.003> PMID: 22325892
66. Li J, Islam F, Huang Q, Wang J, Zhou W, Xu L, et al. Genome-wide characterization of WRKY gene family in *Helianthus annuus* L. and their expression profiles under biotic and abiotic stresses. *PLOS ONE.* 2020; 15: e0241965. <https://doi.org/10.1371/journal.pone.0241965> PMID: 33270651
67. Li Q, Yan J. Sustainable agriculture in the era of omics: knowledge-driven crop breeding. *Genome Biol.* 2020; 21: 154. <https://doi.org/10.1186/s13059-020-02073-5> PMID: 32591012
68. Abe S, Sado A, Tanaka K, Kisugi T, Asami K, Ota S, et al. Carlactone is converted to carlactonoic acid by MAX1 in *Arabidopsis* and its methyl ester can directly interact with AtD14 in vitro. *Proc Natl Acad Sci U S A.* 2014; 111: 18084–18089. <https://doi.org/10.1073/pnas.1410801111> PMID: 25425668
69. Zhang D, Qi J, Yue J, Huang J, Sun T, Li S, et al. Root parasitic plant *Orobancha aegyptiaca* and shoot parasitic plant *Cuscuta australis* obtained *Brassicaceae*-specific strictosidine synthase-like genes by horizontal gene transfer. *BMC Plant Biol.* 2014; 14: 19. <https://doi.org/10.1186/1471-2229-14-19> PMID: 24411025
70. Wakabayashi T, Hamana M, Mori A, Akiyama R, Ueno K, Osakabe K, et al. Direct conversion of carlactonoic acid to orobanchol by cytochrome P450 CYP722C in strigolactone biosynthesis. *Sci Adv.* 2019; 5: eaax9067. <https://doi.org/10.1126/sciadv.aax9067> PMID: 32064317
71. Yoneyama K, Mori N, Sato T, Yoda A, Xie X, Okamoto M, et al. Conversion of carlactone to carlactonoic acid is a conserved function of MAX1 homologs in strigolactone biosynthesis. *New Phytol.* 2018; 1522–1533. <https://doi.org/10.1111/nph.15055> PMID: 29479714
72. Trabelsi I, Yoneyama K, Abbas Z, Amri M, Xie X, Kisugi T, et al. Characterization of strigolactones produced by *Orobancha foetida* and *Orobancha crenata* resistant faba bean (*Vicia faba* L.) genotypes and effects of phosphorous, nitrogen, and potassium deficiencies on strigolactone production. *South Afr J Bot.* 2017; 108: 15–22. <https://doi.org/10.1016/j.sajb.2016.09.009>
73. Iseki M, Shida K, Kuwabara K, Wakabayashi T, Mizutani M, Takikawa H, et al. Evidence for species-dependent biosynthetic pathways for converting carlactone to strigolactones in plants. *J Exp Bot.* 2018; 69: 2305–2318. <https://doi.org/10.1093/jxb/erx428> PMID: 29294064
74. Ueno K, Nakashima H, Mizutani M, Takikawa H, Sugimoto Y. Bioconversion of 5-deoxystrigol stereoisomers to monohydroxylated strigolactones by plants. *J Pestic Sci.* 2018; 43: 198–206. <https://doi.org/10.1584/jpestics.D18-021> PMID: 30363087
75. Yoshida S, Shirasu K. Multiple layers of incompatibility to the parasitic witchweed, *Striga hermonthica*. *New Phytol.* 2009; 183: 180–189. <https://doi.org/10.1111/j.1469-8137.2009.02840.x> PMID: 19402875